0026-895X/10/7805-827–836$20.00
MOLECULAR PHARMACOLOGY
Vol. 78, No. 5
65250/3634540
Mol Pharmacol 78:827–836, 2010
Printed in U.S.A.

Auraptene Is an Inhibitor of Cholesterol Esterification and a Modulator of Estrogen Receptors

Philippe de Medina, Salvatore Genovese, Michael R. Paillasse, Mahta Mazaheri, Stephanie Caze-Subra, Kerstin Bystricky, Massimo Curini, Sandrine Silvente-Poirot, Francesco Epifano, and Marc Poirot

Institut National de la Santé et de la Recherche Médicale U-563 (P.d.M., M.R.P., S.S.-P., M.E.P.) and Université Paul Sabatier (S.S.-P., M.P., K.B.), Toulouse, France; Affichem, Toulouse, France (P.d.M., M.R.P.); Laboratoire de Biologie Moléculaire Eucaryote-Centre National de la Recherche Scientifique (M.M., S.C.S., K.B.) and Dipartimento di Scienze del Farmaco (S.G., F.E.), Università "G. D'Annunzio," Chieti-Pescara, Chieti Scalo, Italy; and Dipartimento di Chimica e Tecnologia del Farmaco, Sezione di Chimica Organica, Università degli Studi di Perugia, Perugia, Italy (M.C.)

Received April 8, 2010; accepted August 11, 2010

ABSTRACT

Auraptene is a prenyloxycoumarin from *Citrus* species with chemopreventive properties against colitis-related colon and breast cancers through a yet-undefined mechanism. To decipher its mechanism of action, we used a ligand-structure based approach. We established that auraptene fits with a pharmacophore involved in both the inhibition of acyl-CoA:cholesterol acyl transferase (ACAT) and the modulation of estrogen receptors (ERs). We confirmed experimentally that auraptene inhibits ACAT and binds to ERs in a concentration-dependent manner and that it inhibited ACAT in rat liver microsomes and in intact cancer cells of murine and human origins, with an IC_{50} value in the micromolar range. Auraptene bound to ERs with affinities of 7.8 μM for ERα and 7.9 μM for ERβ, stabilized ERs, and modulated their transcriptional activity via an ER-dependent reporter gene and endogenous genes. We further established that these effects correlated well with the control of growth and invasiveness of tumor cells. Our data shed light on the molecular mechanism underlying the anticancer and chemopreventive effects of auraptene.

Introduction

Auraptene (7-geranyloxycoumarin) is the most abundant prenyloxycoumarin found (Curini et al., 2006) in plants of the genus *Citrus* (Epifano et al., 2008). Various dietary components such as marmalades and grapefruit-derived products, such as juices, can contain significant amounts of auraptene, ranging from 0.11 to 0.38 mg/100 g in fresh products (Ogawa et al., 2000). Dietary administration of auraptene to animals has revealed numerous pharmacological activities. Auraptene induces anti-inflammatory, antioxidant, antibacterial, and immunomodulatory effects (Epifano et al., 2008). It is noteworthy that auraptene has been shown to protect rodents against chemically induced carcinogenesis (Tanaka et al., 1998, 2000, 2010; Kohno et al., 2006; Krishnan et al., 2009). It has also been reported to exert antiproliferative and proapoptotic activities on cancer cell lines such as human hepatocellular carcinoma, colorectal adenocarcinoma, and breast adenocarcinoma cells in vitro (Zheng et al., 2002; Ohnishi et al., 2004; Krishnan et al., 2009). As a consequence, auraptene is potentially very interesting as a dietary chemopreventive agent for cancers. To date, little is known about the molecular mechanisms involved in the chemopreventive activity of auraptene against cancer or about its cellular effects.

The chemopreventive and the anticancer actions of au-

This study was supported by the Institut National de la Santé et de la Recherche Médicale; the Conseil Regional Midi-Pyrénées; the Institut National du Cancer through the ResisTH network; and Affichem. S.S.-P. is in charge of research at the Centre National de la Recherche Scientifique.

Article, publication date, and citation information can be found at http://molpharm.aspetjournals.org.

doi:10.1124/mol.110.065250.

ABBREVIATIONS: ER, estrogen receptor; E2, 17β-estradiol; Sah 58-035, 3-[decyldimethylsilyl]-*N*-[2-(4-methylphenyl)-1-phenylethyl]-propanamide; ICI 164,384, [(*N*-*n*-butyl-*N*-methyl-11-[3,17β-di-hydroxy estra-1,3,5(10)-trien-7α-yl]-undecanamide]; TMP-153, *N*-[4-(2-chlorophenyl)-6,7-dimethyl-3-quinolyl]-*N′*-(2,4-difluorophenyl)urea; CE, cholestan-5α,6α-epoxy-3β-ol; ACAT, acyl-CoA:cholesterol-acyl transferase; TLC, thin-layer chromatography; SERM, selective estrogen receptor modulator; AEBS, antiestrogen binding site; ChEH, cholesterol-5,6-epoxide hydrolase; Tam, tamoxifen; FBS, fetal bovine serum; FCS, fetal calf serum; DMEM, Dulbecco's modified Eagle's medium; OH-Tam, 4-hydroxytamoxifen; PBS, phosphate-buffered saline; RT-PCR, reverse transcriptase polymerase chain reaction; PR, progesterone receptor; TGFα, transforming growth factor α.

raptene suggest that it modulates one (or more) target involved in the control of oncogenic processes. Our attention has been drawn to the targets of tamoxifen (Tam), a drug that has been in use for more than 30 years for the treatment and prevention of estrogen receptor (ER)-positive breast cancers (Jordan, 2007) and that has a complex pharmacology for which several targets have been identified. In addition to binding to ERs (Jensen and Jordan, 2003), Tam has been shown to inhibit cholesterol esterification (de Medina et al., 2004, 2006; Payré et al., 2008) and to bind to the antiestrogen binding site (AEBS) with high affinity (Kedjouar et al., 2004). These additional targets account for the pharmacology of Tam (de Médina et al., 2004) and are involved in its anticancer and chemopreventive activities (Payré et al., 2008; de Medina et al., 2009a,b). Through a direct genomic mechanism, Tam modulates the transcription of genes under the control of ERs. ER modulators can produce a transcriptional signature that will differ according their chemical structure (McDonnell et al., 1995) and will affect the functionality of ERs by controlling their subcellular localization and stabilization (Wittmann et al., 2007). SERM have been shown to block the mitogenic action of low doses of 17β-estradiol (E2) and to prevent against the occurrence of ER(+) breast cancers (Jordan, 2004). More recently, the importance of ERs in the cause of colonic cancers was proposed, and it was shown that ER modulation could reduce the formation of preneoplastic lesions in the colon (Weige et al., 2009) and control colon cancer, cell proliferation, and death (Xu and Thomas, 1994; Booth et al., 1999; Janakiram et al., 2009) showing that ER modulation could prevent the occurrence of colonic cancer.

We have reported that Tam inhibited the Acyl-CoA:Cholesterol Acyl Transferase (ACAT) activity in macrophages and tumor cell lines (de Médina et al., 2004; de Medina et al., 2004, 2006; Payré et al., 2008). It is noteworthy that cholesteryl esters have been reported to accumulate in tumors and to be involved in cell proliferation and invasiveness that are blocked by the inhibition of ACAT (Tosi and Tugnoli, 2005; Paillasse et al., 2009). The AEBS is a hetero-oligomeric proteinaceous binding site made up of multifunctional enzymes involved in cholesterol metabolism (Kedjouar et al., 2004) that include cholesterol-5,6-epoxide hydrolase activity (ChEH) (de Medina et al., 2010). We recently showed that Tam induced the differentiation and death of breast cancer cells through the accumulation of cholesterol precursors and cholesterol oxidation products (Payré et al., 2008; de Medina et al., 2009a,b). We have also done structure-function studies that allowed us to identify pharmacophores involved in the inhibition of ACAT (de Medina et al., 2004b), ER modulation (de Medina et al., 2006), and AEBS binding (Poirot et al., 2000). The structure of auraptene led us hypothesize that it might modulate some of these targets of Tam, which may explain its action in chemoprevention and cell growth control.

In the present article, we have compared auraptene with pharmacophores that target ERs, ACAT, and the AEBS and characterized its effect on different tumor cell lines. We show that auraptene is a modulator of ERs and an inhibitor of cholesterol esterification.

Materials and Methods

Chemicals. [^{3}H]17β-Estradiol, [^{3}H]tamoxifen, [^{14}C]oleyl-CoA, and [^{14}C]cholesterol were purchased from GE Healthcare (Chalfont St. Giles, Buckinghamshire, UK). The radiochemical purity of the compounds was verified by thin-layer chromatography (TLC) and was greater than 98%. [(*N*-*n*-Butyl-*N*-methyl-11-[3,17β-dihydroxyestra-1,3,5(10)-trien-7α-yl]-undecanamide] (ICI 164,384) was provided by Zeneca Pharmaceuticals plc (Macclesfield, UK). *N*-[4-(2-Chlorophenyl)-6,7-dimethyl-3-quinolyl]-*N*′-(2,4-difluorophenyl)urea (TMP-153) was from Enzo Life Sciences (Plymouth Meeting, PA). 3-[decyldimethylsilyl]-*N*-[2-(4-methylphenyl)-1-phenylethyl]-propanamide (Sah 58-035) was kindly provided by A. Suter at Novartis (Basel, Switzerland). 7-Geranyloxycoumarin (auraptene) and 7-hydroxycoumarine (umbelliferone) were synthesized as described previously (Curini et al., 2004). Other compounds and chemicals were from Sigma-Aldrich (St. Louis, MO), solvents from VWR (Fontenay sous Bois, France), and TLC plates were obtained from Whatman (Clifton, NJ).

Molecular Structure Analysis. The structure analysis and the comparisons between the structure of compounds was done exactly as described previously (de Medina et al., 2006). Superimposition of the energy-minimized structure of auraptene and the active structures of Sah 58-035 and ICI 164,384 was done by superimposing the benzopyrone ring of auraptene on the tolylethanamine part of the diphenyl ethane backbone of Sah 58-035 and rings A and B of the steroid backbone of ICI 164,384, respectively. For the superimposition with ICI 164,384, carbon 3 of the phenyl ring of the steroid was adjusted to carbon 3 of the benzopyrone part of auraptene, and the benzylic carbon linked to carbon 6 of the phenyl of the steroid was superimposed on carbon 7 of the oxycoumarin part of auraptene. For the superimposition with Sah 58-035, carbon 4 of the diphenyl ethane part of Sah 58-035 was adjusted to carbon 3 of the oxycoumarin part of auraptene, and the benzylic carbon of the phenyl of the diphenyl ethane of Sah 58-035 was superimposed on carbon 7 of the oxycoumarin part of auraptene. The percentage of superimposition was calculated by measuring the ratio of the intersection of the van der Waals volume of the compounds with the van der Waals volume of the diphenyl ethane of Sah 58-035.

Assays for ACAT Activity. Rat liver microsomes were prepared as described previously (de Medina et al., 2004b). The 105,000*g* microsomal pellet was resuspended in 0.1 M phosphate buffer, pH 7.4, 1 mM EDTA, and 2 mM dithiothreitol at a protein concentration of 5 mg/ml. The ACAT activity was assayed by measuring the formation of cholesteryl [^{14}C]oleate from the endogenous cholesterol in the microsomal fraction and exogenous [^{14}C]oleyl-coA as the substrate, following the procedure described previously (de Medina et al., 2004b). The ACAT activity was expressed as the percentage of the activity measured in the absence of inhibitors (control assay with solvent vehicle). The ACAT control was 48.3 $\pm$ 2.3 pmol of cholesteryl [^{14}C]oleate $\cdot$ mg protein^{-1} $\cdot$ min^{-1} and the background represented less than 1% of the specific signal. ACAT activity was assayed using 40 μM [^{14}C]oleyl-CoA in the presence or absence of 1, 5, 10, 25, and 50 μM concentrations of the tested compounds. The concentration of compound required to inhibit ACAT by 50% (IC_{50}) was calculated using Prism software, version 4.0 (GraphPad Software Inc., San Diego, CA). The IC_{50} values were calculated with data from triplicate assays at each drug concentration.

Cell Culture. SW-620, MDA-MB-231, and MCF-7 cells were from the American Type Culture Collection (Manassas, VA), and NIH-3T3 and CCK2R-E151A cells (E151A) were obtained as described previously (Galés et al., 2003). SW-620 and MCF-7 were, unless otherwise indicated, routinely grown in RPMI 1640 growth medium containing 5% fetal bovine serum (FBS) (Invitrogen, Carlsbad, CA), 2 mM glutamine, and 50 U/ml penicillin, and 50 U/ml streptomycin. E151A were grown in DMEM containing 10% FBS, 2 mM glutamine, and 50 U/ml of both penicillin and streptomycin. Cells were incubated at 37°C in a humidified 5% CO_2/air atmosphere.

Assay for ACAT Activity in Intact Cells. SW-620, MDA-MB-231, E151A, and MCF-7 cells were plated on six-well plates (40,000 cells/well). ACAT activity in intact cells was measured as described previously (Paillasse et al., 2009). Cells were preincubated for 15 min

with solvent vehicle or increasing concentrations of auraptene or Sah 58-035 ranging from 0.1 to 100 μM in complete medium. [^{14}C]Cholesterol (0.2 μCi/well) was added, and the cells were incubated for 24 h. At the end of the incubation, intracellular and secreted lipids in the supernatant were extracted and then separated by TLC as described previously (Paillasse et al., 2009). Free and esterified cholesterol were identified using purified ^{14}C commercial standards, and the radioactivity of each individual lipid was quantified using a phosphor screen (Storm; GE Healthcare). The ACAT activity was expressed as the percentage of the ACAT activity measured in the absence of inhibitors (cells were treated with solvent vehicle).

Molecular Modeling with Estrogen Receptors. Molecular modeling experiments were conducted exactly as described previously (de Medina et al., 2006).

Estrogen Receptor Binding Assay. Competition binding to ERα and ERβ was measured exactly as described previously (de Medina et al., 2006).

Reporter Cell Lines and Luciferase Assay. MELN cells expressed luciferase in an estrogen-dependent manner, and MRLN cells expressed luciferase in a retinoid-dependent manner (de Medina et al., 2006). Cells were routinely grown in RPMI 1640 growth medium and MELN in DMEM, supplemented with 5% FBS. For experiments, cells were grown for 5 days in phenol red-free medium containing 5% dextran-coated charcoal-treated FBS. Luciferase assay were carried out exactly as described previously (de Medina et al., 2006).

Microsomal Antiestrogen Binding Site and ChEH Assays. Competition of binding to the rat liver microsomal AEBS was measured exactly as described previously (Payré et al., 2008). Inhibition of ChEH activity was measured as described previously on a whole-cell assay using MCF-7 cells (de Medina et al., 2010). [^{14}C]α-CE (10 Ci/mol) was synthesized as described previously (de Medina et al., 2010). Cells were treated for 24 h with 0.6 μM [^{14}C]α-CE. The final assay volume was 150 μl of with 130 μl of buffer (50 mM Tris, pH 7.4, and 150 mM KCl), 10 μl of microsomal proteins (15 mg/ml), and 10 μl of acetonitrile (6.7%) containing the test compound/drug and the labeled α-CE. Tubes were incubated at 37°C for increasing periods of time from 0 to 30 min. The reaction was stopped by immersing the samples in ice water and adding 1.5 ml of chloroform/methanol (2:1) and 500 μl of reaction buffer. After shaking, the lower phase was removed and saved, and the aqueous phase was extracted with 1.5 ml of chloroform. The two organic layers were mixed, reduced to dryness under a flux of nitrogen, and the residue was resuspended in 60 μl of ethanol. More than 95% of the radioactivity was recovered in the organic layers. Samples were applied to TLC plates that had been heated previously for 1 h at 100°C and were developed using ethyl acetate. The regions corresponding to authentic CE and cholestane-3β,5α,6β-triol standards were visualized by iodine vapor. Radioactive metabolites were visualized using a Storm apparatus (GE Healthcare) and quantified by densitometry with the software ImageQuant (GE Healthcare).

Cell Fractionation and Western Blot Analysis. MCF-7 cells were treated with solvent vehicle (ethanol or dimethyl sulfoxide), 10 nM E2, 1 μM 4-hydroxytamoxifen (OH-Tam), 1 μM ICI 164,384, or 25 μM auraptene for 3 h. The cell fractionation protocol was adapted from Wittmann et al. (2007) as follows: cells were treated and washed with ice-cold PBS, scraped, and centrifuged at 300*g* for 10 min at 4°C. The pellets were resuspended in 100 μl of cytoplasmic extraction buffer at 25°C [10 mM HEPES, pH7.3, 10 mM KCl, 0.1 mM EDTA, 0.1 mM EGTA, 0.63% NP-40 (IGEPAL), 1 mM dithiothreitol, and protease inhibitor cocktail], kept 15 min on ice, vortexed for 10 s, and centrifuged at 15,000*g* for 5 min at 4°C to obtain the cytosolic fraction (C). The pellets were resuspended in 100 μl of nuclear soluble buffer (20 mM HEPES, pH 7.3 at 25°C, 10% glycerol, 0.5 M NaCl, 1 mM EDTA, 1 mM EGTA, 1 mM dithiothreitol, and protease inhibitor cocktail), incubated for 30 min at 4°C, vortexed, and centrifuged at 15,000*g* for 5 min at 4°C to obtain the soluble nuclear fraction (S). The last pellets were resuspended in 100 μl of nuclear insoluble buffer (95% Laemmli buffer and 5% β-mercaptoethanol) and incubated for 5 min on ice before boiling them for 20 min at 95°C to obtain the insoluble nuclear fraction (I). The different fractions were electrophoresed, transferred to nitrocellulose membrane, and subjected to Western blot analysis. The membrane was blotted with the primary polyclonal antibodies anti-human ERα (HC20) and anti-human cytokeratin 18 (H-80) purchased from Santa Cruz Biotechnology (Santa Cruz, CA). The secondary antibody used was alkaline phosphatase-conjugated anti-rabbit immunoglobulin G (Sigma-Adrich). For signal detection, an enhanced chemiluminescence substrate was used (Roche Diagnostics, Indianapolis, IN), and bands observed on a BioImager (Fujifilm, Tokyo, Japan) and quantified using MultiGauge software (Fujifilm).

Quantitative RT-PCR. MCF-7 cells (5×10^6) were grown in phenol red-free medium containing 5% dextran-coated charcoal-treated FBS for 3 days and then incubated with 10 nM E2 in the presence or absence of 1 μM ICI 164,384 or 25 μM auraptene, 25 μM auraptene in the presence or absence of 10 nM E2, or 1 μM ICI 164,384 or solvent vehicle for 16 h. Total RNAs were extracted using TRIzol reagent (Invitrogen) and the quality of the RNA samples assessed by electrophoresis on an agarose gel followed by ethidium bromide staining, in which the 18S and 28S RNA bands could be visualized under UV light. RNA was quantified by spectrophotometry at 260 nm. RNA samples were stored in Rnase-free distilled water at −80°C. Total RNA (1–5 μg) was reverse-transcribed in a final volume of 20 μl of using a SuperScript III Reverse Transcriptase kit (Invitrogen). cDNA was stored at −80°C. All target transcripts were detected using quantitative real-time RT-PCR (SyberGreen) assays. The experiments were performed on a Mastercycler real-plex device, and TBP was used as endogenous control for normalization of the data. The following primer pairs were used to amplify cDNA after reverse transcription: for TBP, 5′-CGGCTGTTTAACTTCGCTTTC-3′ and 5′-CCAGCACACTCTTCTCAGCA-3′; for Ps2/TFF1, 5′-CCCCTGGTGCTTCTATCCTAAT-3′ and 5′-CAGATCCCTGCAGAAGTGT CTA-3′; for PR, 5′-CTTAATCAACTAGGCGAGAG-3′ and 5′-AAGCTCATCCAAGAATA CTG-3′; and for TGFα, 5′-ATCTCTGGCAGTGCTGTCCCT-3′ and 5′-CTTGCTGCCACTCA GAAACA-3′. The thermal cycling conditions comprised 2 min at 55°C and 2 min at 95°C followed by 40 cycles at an appropriate annealing temperature depending on the primer set for 1 min. The results were quantified by the comparative C_t method using qBASE software (available at http://www.qbase.net).

Progesterone Receptor Expression. For each condition, 9×10^5 cells were seeded in 140-mm diameter dishes and treated, as described above, in a final volume of 15 ml. Cells were incubated for 48 h with E2 or auraptene. Quantification of the PR was carried out on the cytosolic fraction of cells exactly as described in a previous article (de Medina et al., 2006). In brief, after treatment, the culture medium was removed, and the cells were washed twice with PBS and scraped into 350 μl of homogenization buffer (10 mM Tris buffer, pH 7.4, containing 20 mM molybdic acid, and 12 mM monothioglycerol). The cells were lysed by three cycles of freeze/thawing (−170 /20°C) and then centrifuged at 100,000*g* for 60 min at 4°C. We used the Abbott progesterone receptor-EIA monoclonal kit, according to the manufacturer's instructions (Abbott, Rungis, France). Cytosolic protein concentrations were measured using the Bradford technique to normalize the progesterone receptor expression data. For each condition, the mean receptor concentration was calculated from the data of two independent dishes.

Proliferation Assays. Cells were seeded in RPMI 1640 with 5% FBS into 12-well plates at 30,000/well and treated for 3 days with 50 μM auraptene or 25 μM Sah 58-035 and 2.5 μM Tam in the presence or absence of 10 nM E2. Drugs and medium were changed after 48 h. For proliferation assays, cells were grown for 5 days in phenol red-free medium containing 5% dextran-coated charcoal-treated FBS. Cells were seeded into 96-well plates at 2000 cells/well. Treatment media (150 μl/well) were added on the following day and replaced at 48-h intervals until the end of the experiment. Cell density was

measured using the tetrazolium reduction assay (Sigma-Aldrich). The absorbance at 540 nm of the formazan was measured directly in the 96-well plates with a Multiscan Multisoft plate reader from Thermo Fisher Scientific (Waltham, MA).

Clonogenic Assay. Cells were trypsinized and plated in 60-mm tissue culture plates at a density of 500 to 1000 per plate. The cells were allowed to adhere for 24 h, and drugs were added to the final concentrations from concentrated stocks. After 24 to 72 h of incubation, the plates were washed twice with serum-free medium, fresh medium was added, and the cells were incubated until colonies were visible. The plates were washed once with PBS and stained with Coomassie brilliant blue. Visible colonies were counted and reported as the percentage of control cells [ethanol-treated, 0.01% (v/v)].

Cell Invasion Assays. Cells were seeded in six-well plates (40,000 cells/well) in DMEM with 10% FCS. After 24 h, the cells were pretreated for 24 h in the presence of the indicated test compounds or vehicle in DMEM with 2% FCS and then harvested and counted. Cells (20,000 cells) were layered in serum-free DMEM on top of Nunc filters (8-mm diameter, 8-μm pore size; Nalge Nunc International, Rochester, NY) coated with growth factor-reduced Matrigel (250 μg/ml Matrigel; BD Biosciences, San Jose, CA) in the presence of the appropriate test compound or vehicle. The bottom of the filter was filled with 10% FCS/DMEM. After 48 h at 37°C, cells that had invaded the Matrigel and were attached to the lower face of the filter were fixed, stained with Giemsa stain, and counted under the microscope.

Statistical Analysis. Values are the mean ± S.E. of three independent experiments, each carried out in duplicate. Statistical analysis was carried out using a Student's *t* test for unpaired variables. * and ** in the figures refer to *P* values of <0.001 and <0.0001, respectively, compared with control cells that received the solvent vehicle alone.

Results

Auraptene shares structural similarities with ACAT inhibitors and ER ligands. The secondary structures of auraptene, Sah 58-035 and ICI 164,384, are depicted in Fig. 1. We have investigated the structural similarities that exist between minimal energy conformations of auraptene and the active conformations of Sah 58-035 and ICI 164,384 in a three-dimensional representation (Fig. 1B). The van der Waals volumes of auraptene, Sah 58-035, and ICI 164,384 were 250, 425, and 469 Å^3, respectively. An overlay of the compounds is shown in Fig. 1C and shows that auraptene shares a common volume of 173.77 and 184.38 Å^3 with Sah 58-035 and ICI 164,384, respectively, 69% of the auraptene volume in common with the ACAT inhibitor, and 73% of the auraptene volume in common with the ER ligand. The hydrophobic side chain of auraptene perfectly superimposes on the side chains of Sah 58-035 and ICI 164,384. The benzopyrone ring of auraptene is planar and superimposes on the tolyl-ethyl-amine group of the diphenylethane backbone of Sah 58-035 and the ring A and B of the steroid backbone of ICI 164,384. These results show that auraptene shares strong three-dimensional structural homologies with compounds with dual functions of inhibitors of ACAT and estrogen receptor ligands (i.e., Sah 58-035 and ICI 164,384).

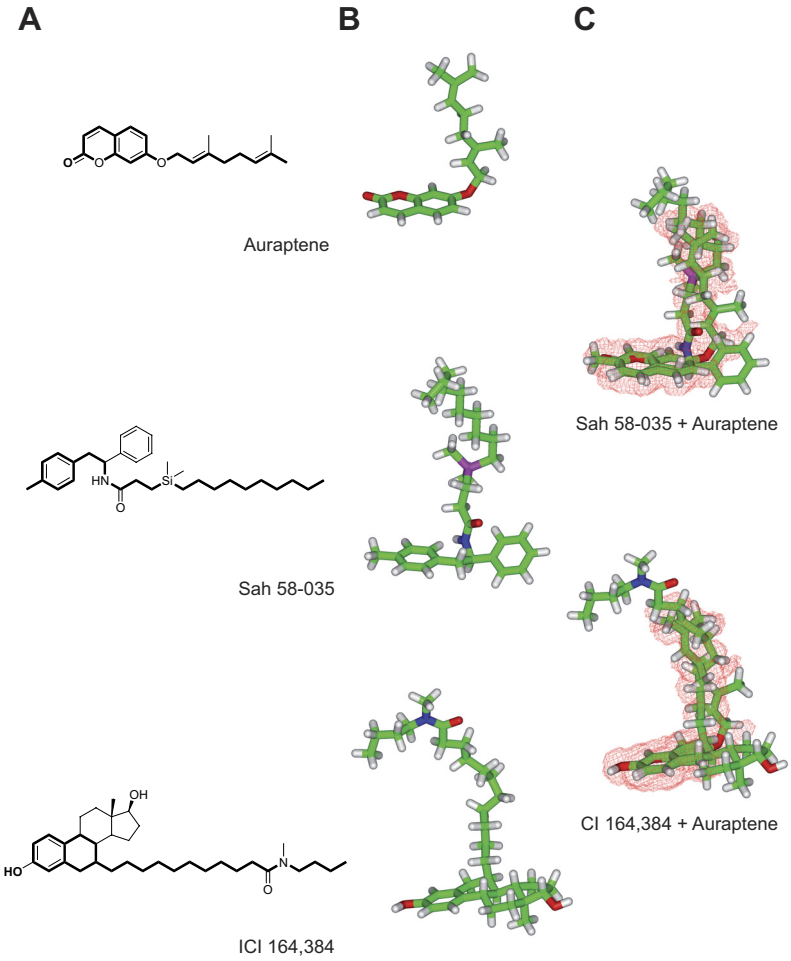

Fig. 1. Chemical structure of auraptene, Sah 58-035, and ICI 164,384. A, the parts of the molecules that are superimposable are in boldface type. B, three-dimensional structures of the calculated minimal energy conformation of auraptene and of the active conformations of Sah 58-035 and ICI 164,384 are shown. The calculated minimal energy was obtained using the Discover module of Insight II. The overlay of auraptene with Sah 58-035 or with ICI 164,384, as well as van der Waals volume calculations and intersection measurements, were done using the Search-Compare module as described under *Materials and Methods*. C, the van der Waals volume intersection is depicted as the red grid and illustrates the structural similarities between auraptene, Sah 58-035, and ICI 164,384. The van der Waals volume of auraptene, SAH 58-035, and ICI 164,384 are 250.05, 425.03, and 468.77 Å^3, respectively. The intersection volume between auraptene and SAH 58-035 is 173.77 Å^3. This gives 69% of the auraptene volume in common with the ACAT inhibitor. The intersection volume between auraptene and ICI 164,384 is 184.38 Å^3 (i.e., 73% of the auraptene volume in common with the ER ligand).

Auraptene Is an Inhibitor of ACAT in Rat Liver Microsomes and Intact Cells. The auraptene inhibition of ACAT in vitro was first measured with rat liver microsomes. Sah 58-035 and ICI 164,384 inhibited ACAT with IC_{50} values of 0.38 ± 0.12 and 0.61 ± 0.22 μM, similar to those reported in the literature (de Medina et al., 2004b), whereas auraptene inhibited ACAT in a concentration-dependent manner with an IC_{50} of 4.18 ± 0.31 μM (Fig. 2A). Umbelliferone, which is an analog of auraptene but lacks the prenyl side chain, did not inhibit ACAT (Fig. 2A). The inhibition of cholesterol esterification was then evaluated with intact cells: auraptene inhibited cholesterol esterification in a concentration-dependent manner with an IC_{50} of 2.37 μM for MCF-7 cells, 3.02 μM for MDA-MB-231 cells, 3.20 μM for SW-620 cells, and 6.94 μM for E151A cells (Fig. 2, B and C), confirming that auraptene inhibited cholesterol esterification in rat liver microsomes and in intact cells in the range of 1 to 10 μM.

Molecular Modeling of the Complex ER α/Auraptene. We then investigated possible interactions of auraptene with ERs by molecular modeling. The docking of auraptene into the ERα taken from the X-ray structure of the complex ER-OH-Tam (Shiau et al., 1998) and energy minimization gave a complex in which the auraptene fitted well into the ligand binding domain (Fig. 3, A and B). In Fig. 3B, chemical interactions between auraptene and the ER are shown. The dihydropyranone part of the benzopyrone ring of auraptene is planar and produced a stacking interaction with the phenyl side chain of Phe404 and van der Waals contacts with the methyl groups of Leu391 and Leu384, as observed for the phenol of estradiol (Brzozowski et al., 1997). The carboxyl group from the pyran-141-one group of auraptene established a hydrogen bond with Arg394 and defined a cluster of van der Waals interactions with the side chains of Glu353 and Leu349. The phenyl ring of the benzopyrone moiety of auraptene made van der Waals contacts with Leu346 and Leu384. These data show that the benzopyrone ring of auraptebfene can occupy the same cavity as E2 or diethylstilbestrol (Brzozowski et al., 1997; Shiau et al., 1998). The side chain of auraptene protrudes into the 11β cavity of the ligand binding domain of the ER and produced multiple van der Waals interactions with hydrophobic amino acids such as Ala350, Leu525, and Trp383. No interaction could be observed between auraptene and Asp351, which is involved in the antiestrogenic activity of SERMs such as raloxifene (Levenson and Jordan, 1998). Our molecular model shows strong similarities with those described for the partial estrogen receptor agonist Sah 58-035 (de Medina et al., 2006). Indeed, both compounds fit well with the ERα taken from the X-ray structure of the complex ER-OH-Tam, and no interactions with Asp351 were observed for auraptene and Sah 58-035. These studies established that auraptene was well accommodated within the ligand binding site of the ER, thus reinforcing the results of our binding experiments.

Auraptene Binds to the Estrogen Receptors but Has No Detectable Affinity for the AEBS and Does Not Inhibit ChEH. We next examined whether auraptene interacted with ERs in competition binding assays with [^{3}H]E2. We found that auraptene bound to both ERα and ERβ in a concentration-dependent manner (Fig. 3C), with IC_{50} values of 7.8 and 7.9 μM, respectively. By contrast, auraptene did not bind to the AEBS (Fig. 3C) and does not inhibit ChEH (Fig. 3C) carried out by the AEBS. These data established that auraptene is a ligand of ER with no subtype-selectivity and has no affinity for the AEBS.

A

Compound	IC_{50}
	μM
Sah 58-035	0.38 ± 0.12
ICI 164,384	0.61 ± 0.22
Auraptene	4.18 ± 0.31
Umbelliferone	N.M.

B

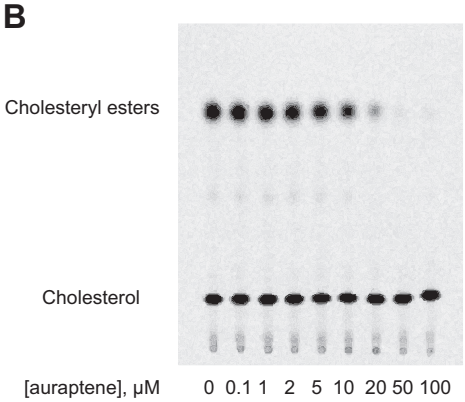

C

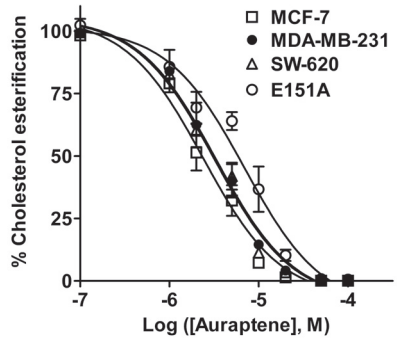

Fig. 2. A, the effect of Sah 58-035, ICI 164,384, auraptene, and umbelliferone on cholesterol esterification (ACAT activity) in rat liver microsomes. Rat liver microsomes (60 μg of protein) were incubated with 10 different concentrations of each drug and 40 μM [^{14}C]-oleyl-CoA. Cholesteryl esters were quantified as described under *Materials and Methods*. The ACAT activity was expressed as the percentage of the ACAT activity measured in the absence of inhibitors (control with solvent vehicle). Curves were analyzed using the curve-fitting program GraphPad Prism (version 4.0). Values are the average of three experiments ± S.E.M., each carried out in duplicate (in some cases, S.E.M. values were less than the size of the symbol, and the error bars are not visible). B, representative autoradiograph of the dose-dependent inhibition of cholesterol esterification by auraptene in RCCK2-E151A (E151A) cells. Cells were incubated with solvent vehicle (control) or auraptene at the indicated concentrations for 24 h in the presence of [^{14}C]cholesterol (0.2 μCi/well). Synthesized cholesterol esters were separated by thin-layer chromatography after labeling of the cells with [^{14}C]cholesterol as described under *Materials and Methods*. The positions of free and esterified cholesterol were determined using ^{14}C standards. C, auraptene inhibition of ACAT activity in MCF-7 cells (□), MDA-MB-231 (●), SW-620 (△), and E151A (○). Cells were treated as described in the legend to Fig. 3A. Free and esterified cholesterol were quantified as described under *Materials and Methods*. The ACAT activity was expressed as the percentage of the ACAT activity measured in the absence of inhibitors (control with solvent vehicle). Curves were analyzed using the curve-fitting program GraphPad Prism (version 4.0). Values are the average of three experiments ± S.E.M., each carried out in duplicate (in some cases, S.E.M. values were less than the size of the symbol, and the error bars are not visible).

Effect of Auraptene on the Cellular Distribution of Estrogen Receptor α. We next evaluated the effect of auraptene on the stability of ERα and its distribution in MCF-7 cells. Cells were fractionated into cytoplasmic, nuclear-soluble, and nuclear-insoluble fractions (Fig. 3D). In the presence of E2, OH-Tam, and auraptene, the ERα was translocated from the cytoplasm to the nuclear fractions (approximately 20% of the total cellular ER). The nuclearization of the ER showed that the interaction between auraptene and the receptor was functional. By contrast, in the presence of ICI, the ER was enriched in the nuclear-insoluble fraction compared with solvent vehicle-treated cells (Fig. 3D). These data established that, similarly to SERMs, auraptene induces nuclear relocalization of the ERα.

Auraptene Is a Partial Agonist of Estrogen Receptor-Dependant Transcription. The ability of auraptene to bind to ERs raised the possibility that it might act as an ER agonist or antagonist, and so we decided to evaluate experimentally the agonist/antagonist properties of auraptene. We used MCF-7 cells stably transfected with a plasmid encoding an estrogen-responsive promoter fused to the luciferase gene that were called MELN (de Medina et al., 2006). Auraptene stimulated the expression of luciferase in MELN cells in a concentration-dependent manner with an EC_{50} of 3.6 ± 1.1 μM and reached a plateau at 20 μM (Fig. 4A), representing 51% of the maximal response observed with E2 (Fig. 4B). This agonist activity was observed in a range of concentrations consistent with the binding affinity of auraptene to the ER, and this stimulation was inhibited by cotreatment with the antiestrogen ICI 164,384 (Fig. 4B). Transient expression experiments in COS-7 cells showed that auraptene was an agonist of ER-dependent expression of luciferase with equal potency on the ERα and ERβ subtypes (data not shown).

Auraptene Modulates the Expression of Endogenous Estrogen Receptor-Regulated Genes. To determine whether auraptene could modulate the expression of endogenous E2-regulated genes and reporter genes, the expression of the PR, TFF1 (Ps2), and TGFα were measured by quantitative RT-PCR in MCF-7 cells treated with or without auraptene (20 μM) or E2. Figure 4C shows that auraptene slightly modulated the transcription of TGFα (×1.1) and inhibited the expression of Ps2 (×0.5). In addition, we showed that auraptene antagonized the stimulation by E2 of Ps2 and TGFα expression with IC_{50} values of 4.50 ± 0.9 and 3.38 ± 0.8 μM, respectively (Fig. 4D). Auraptene stimulated the expression of PR at the mRNA (Fig. 4C) and at the protein levels (Fig. 4E). These data established that auraptene is a modulator of the transcription of genes that are known to be under the control of ER.

Auraptene Controls the Proliferation of Tumor Cell Lines and Blocks the Invasiveness and Colony Formation of Tumor Cells. We next evaluated the effect of auraptene on the proliferation and invasiveness of cell lines. Auraptene induced concentration-dependent growth control

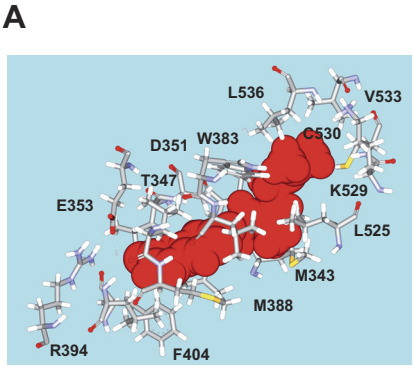

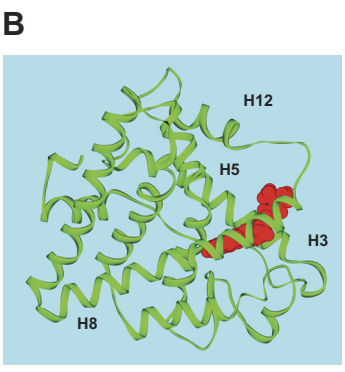

C

Compound	ERα (IC_{50})	ERβ (IC_{50})	AEBS (IC_{50})	ChEH (IC_{50})
	nM	nM	nM	nM
E2	0.8 ± 0.1	1.1 ± 0.1	N.M.	N.M.
Sah 58-035	2,944 ± 412	3,128 ± 204	N.M.	N.M.
Tamoxifen	42.4 ± 0.4	31.9 ± 0.5	12.3 ± 0.2	128 ± 9
Auraptene	7,785 ± 1,202	7,937 ± 1,364	N.M.	N.M.
Umbelliferone	N.M.	N.M.	N.M.	N.M.

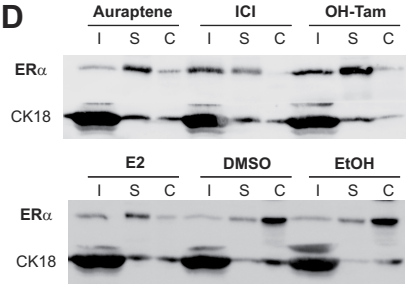

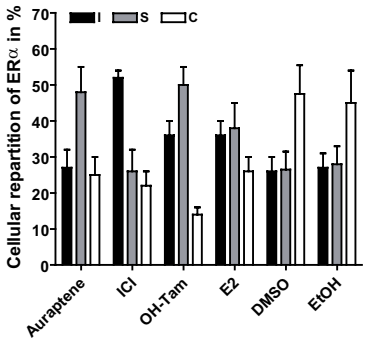

Fig. 3. A, cross-sectional view of the auraptene interactions with the ERα ligand binding domain. Red, auraptene. Amino acid side chains that interact with auraptene are represented. Gray, carbon atoms; white, hydrogen atoms; red, oxygen atoms; blue, nitrogen atoms; yellow, sulfur atoms. B, ribbon representation of the molecular model of auraptene bound to the ERα. Auraptene is drawn in stick form and colored in red. Helical elements or the ER is numbered (H3, H5, H8, and H12) and colored in green. C, binding of auraptene and umbelliferone to ERs, AEBS, and inhibition of ChEH. Binding of radiolabeled E2 to the ERα and ERβ or tritiated tamoxifen to the AEBS were measured at different concentrations of E2, Sah 58-035, auraptene, or umbelliferone as described under *Materials and Methods*. For the ChEH inhibition tests, 150 μg of rat liver microsomal proteins and 10 and 20 μM concentrations of [14C]α-CE with increasing concentrations of compounds ranging from 0.01 to 1000 μM were used under the conditions described under *Materials and Methods*. N.M., no measurable inhibition up to the maximal concentration of inhibitor used. Values are the mean ± S.E.M. from three independent experiments. N.M., no measurable inhibition of binding. D, auraptene induces a stabilization and a relocalization of ERα in the soluble nuclear fractions of MCF-7 cells. MCF-7 cells were grown as described under *Materials and Methods* and treated with either solvent vehicle (EtOH, dimethyl sulfoxide), 100 nM E2, 100 nM ICI 164, 384 (ICI), 100 nM 4-hydroxy-tamoxifen (OH-Tam), or 25 μM auraptene for 3 h. After treatment, cells were harvested and lysed to obtain separated soluble cytoplasmic fractions (C), soluble nuclear fractions (S), and insoluble nuclear fraction (I) as described under *Materials and Methods*. Fractions were subjected to Western analysis to detect ERα and cytokeratin 18. The Western blot is representative of three independent experiments. The percentage of ERα was determined by densitometry using ImageQuant and comparing ERα density in each fraction with the sum of ERα density found in the three fractions.

(Fig. 5A) through an arrest of the cell cycle in the G_0–G_1 phase in the four tumor cell lines (Fig. 5B), showing that auraptene inhibited both the proliferation of ER+ (MCF-7) and ER− (MDA-MB-231) human breast cancer cells; it inhibited the stimulation of MCF-7 proliferation by E2 as observed with estrogen antagonists (Fig. 5C). In addition, Fig. 5D shows that auraptene reduced cell survival in a clonogenic assay causing a 50, 69, 68, and 70% reduction in the number of colonies of MCF-7, MDA-MB-231, SW-620, and E151A cells, respectively. Moreover, auraptene inhibited the motility of these cells, showing that it can inhibit invasiveness (Fig. 5E). These data establish that auraptene reduces the proliferation, viability, and invasiveness of tumor cells of different origins.

Discussion

In this study, we report the identification of two molecular targets of auraptene that explains its chemopreventive and

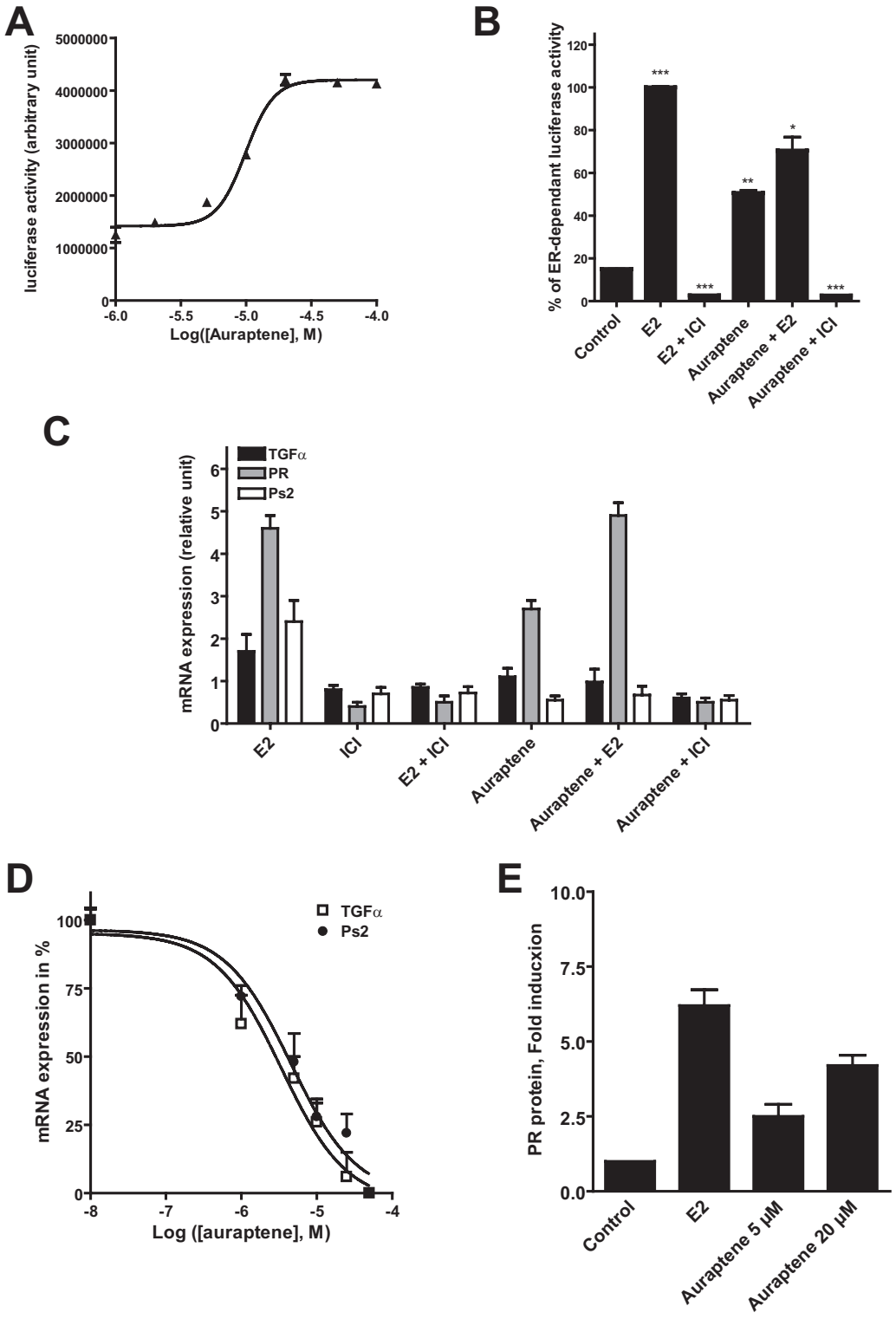

Fig. 4. A, dose-response curve of auraptene on MCF-7 cells stably transfected with ERE-β-globin-tk-Luc (MELN cells) as described under *Materials and Methods*. Results are represented as the ER-dependent luciferase activity obtained with 10 nM E2. B, ER-dependent transcriptional modulatory activity of auraptene on MELN cells. Cells were incubated with solvent vehicule, 1 μM concentration of the antiestrogen ICI 164,384 (ICI), 10 nM E2, or 50 μM auraptene with or without 10 nM E2 or with 50 μM auraptene in combination with 1 μM antiestrogen ICI 164,384 and assayed for luciferase activity. C, auraptene modulated the expression of endogenous genes under the control of ER. Cells were treated with solvent vehicle, 10 nM E2, 1 μM ICI, 1 μM OH-Tam, or 20 μM auraptene with or without 10 nM E2. The relative expression of TGFα, PR, and Ps2 was analyzed by quantitative RT-PCR. Data shown are the mean values ± S.E.M. from three independent experiments. D, dose-response curve of auraptene on MCF-7 cells on the expression of Ps2 and TGFα expression after stimulation with E2. MCF-7 cells were treated with 10 nM E2 and increasing concentrations of auraptene ranging from 10 nM to 50 μM and assayed for TGFα and Ps2 expression by quantitative RT-PCR. E, auraptene stimulated the expression of progesterone receptors. Cells were treated for 48 h with solvent vehicle, 10 nM E2, and 5 and 10 μM auraptene. Analyses were performed as described under *Materials and Methods*. Results are expressed as the ratio of the amount of PR protein in treated cells versus the amount in solvent vehicle-treated cells. Error bars, mean values ± S.E.M. from three independent experiments.

anticancer properties. Using a pharmacophore approach, we hypothesized that auraptene could be both an inhibitor of cholesterol esterification and a modulator of ERs, and this was confirmed experimentally. Auraptene was a potent ACAT inhibitor with liver extracts and intact tumor cells, suggesting that cholesterol esterification is part of its mechanism of action and was a direct estrogen receptor modulator. No affinity for the AEBS was observed, consistent with the absence of the required protonatable dialkylaminoethoxy side chain on auraptene (de Médina et al., 2004). Consis-

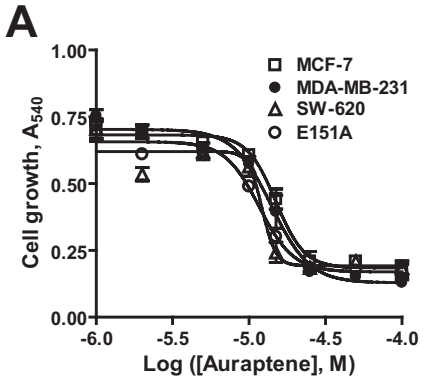

B

	Control				Auraptene			
	pre-G1	G0-G1	S	G2+M	pre-G1	G0-G1	S	G2+M
MCF-7	0	43 ± 1	48 ± 1	9 ± 2	3 ± 1	83 ± 1	7 ±1	7 ± 2
MB-231	0	47 ± 1	45 ± 1	8 ± 2	4 ± 1	79 ± 1	11 ± 1	6 ± 2
SW-620	0	63 ± 1	29 ± 1	8 ± 1	7 ± 1	81 ± 1	7 ±1	5 ± 2
E151A	0	67 ± 2	26 ± 1	7 ± 1	6 ± 1	86 ± 2	8 ± 1	6 ± 2

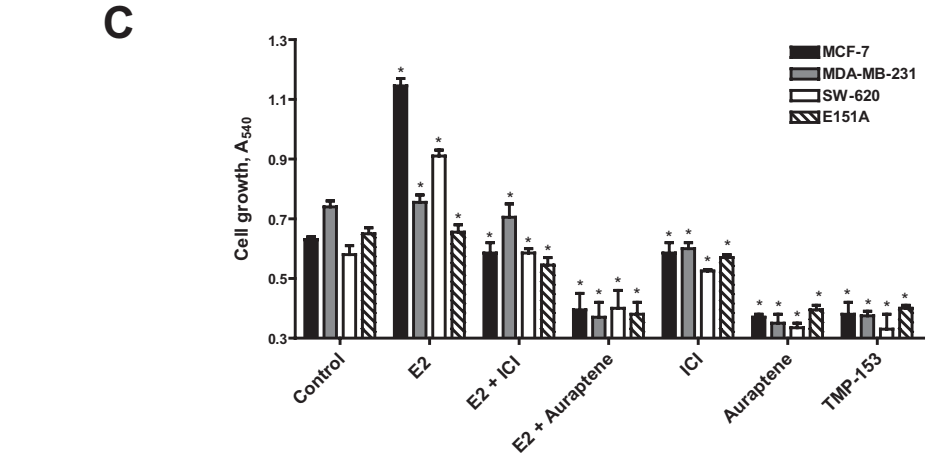

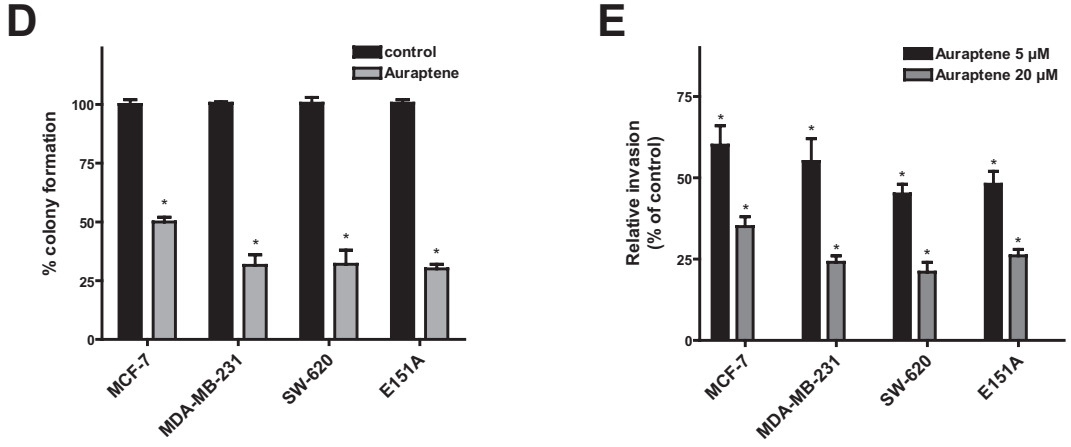

Fig. 5. Effect of auraptene on estrogen- and nonestrogen-regulated growth and invasiveness of MCF-7, MDA-MB-231, SW-620, and RCCK2-E151A cells. A, cells were treated with increasing concentrations of auraptene ranging from 1 to 100 μM. Cell growth was determined as described under *Materials and Methods*. Each point represents the mean values ± S.E.M. B, cell cycle distribution of MCF-7, MDA-MB-231, (MB-231), SW-620, and RCCK2-E151A (E151A) treated with 50 μM auraptene over 48 h. Cell cycle distribution was measured as described under *Materials and Methods* by FACS flow analysis using the BD Biosciences FACS system. C, comparison of the treatment of estrogen-sensitive cells (MCF-7 and SW-620) and estrogen-unresponsive cells (MDA-MB-231 and E151A) with E2 and auraptene with or without pure antiestrogen ICI 164,384, 1 μM ICI 164,384 alone, 25 μM auraptene alone, or 10 μM TMP-153 alone. Values are the mean ± S.E.M. of three separate experiments. D, effect of auraptene on colony formation. Cells were treated with solvent vehicle or 20 μM auraptene, and the number of colonies was measured compared with solvent vehicle-treated cells (taken to be 100%). E, after 24 h of pretreatment with either the solvent vehicle or 25 μM auraptene, cell invasion was assayed using Matrigel-coated filters as described under *Materials and Methods*. After 48 h, cells on the lower surface of the filters were stained and counted under a phase-contrast microscope. For C, D, and E, values are expressed relative to those of cells treated with the solvent vehicle (control) and are the mean ± S.E.M. of three to six separate experiments performed in triplicate.

tently with its lack of affinity for the AEBS, auraptene did not inhibit the cholesterol-5,6-epoxide hydrolase activity, which is carried out by the AEBS. Because auraptene bound to ERs with micromolar affinities and modulated the transcription of reporter and endogenous genes under their transcriptional control, we established that it stimulates the expression of the progesterone receptor but acted as an antagonist to the expression of TGF-α or Ps2. Moreover, auraptene brought about the relocalization of ERs from the cytoplasm to the nucleus as observed with E2 and SERMs. Auraptene did not stimulate the growth of ER-expressing cells, showing that it showed one of the expected properties of a SERM in that it acts as an antagonist on TGF-α expression and sustains the lack of mitogenicity on estrogen-responsive cells. This makes it unlikely that auraptene risks causing endometrial cancer development, as observed with certain SERMs such as tamoxifen (Jordan, 2003). The involvement of ERs in the anti-inflammatory properties of aurapene (Epifano et al., 2008) deserves further investigation.

In vitro tests with auraptene are usually conducted at concentrations ranging from 10 to 50 μM (Epifano et al., 2008). At these concentrations, both ER modulatory activity and ACAT inhibition occurred. Auraptene is well tolerated in rodents and does not show any toxicity up to 1000 mg/kg (Tanaka et al., 2000). When used at 500 ppm (40 mg/kg) as a dietary additive, it has been shown to be present in the mammary glands of treated animals at concentrations ranging from 0.5 to 3.5 μM (Krishnan et al., 2009). Given that the IC_{50} values of the regulation of ER-dependent transcription in our study were 3.5 and 4.5 μM, ER modulation will be fully obtained at pharmacological concentrations in auraptene. It is noteworthy that auraptene acts as an antagonist of TGFα expression, blocking a mitogenic pathway involving EGF receptor signaling. Auraptene inhibits ACAT in intact cells at pharmacological concentrations. Both mechanisms are relevant to the anticancer and chemopreventive properties of auraptene. Estrogens were shown to stimulate proliferative pathways involving signaling pathways such as TGFα signaling, and cholesteryl esters have been reported to accumulate in cells and to stimulate cell proliferation and invasiveness (Paillasse et al., 2009). It is noteworthy that both SERMs and ACAT inhibitors have been reported to induce cell cycle inhibition through the inhibition of the expression of cyclin D1 (Batetta et al., 2003; Renoir et al., 2008). ACAT inhibition may lead to the accumulation of free oxysterols that can inhibit cyclin-D1 expression and inhibit human breast cancer cell proliferation through the oxysterol receptors LXR (Vedin et al., 2009), which are widely expressed in tumor cell lines (Holbeck et al., 2010). This mechanism can contribute to the antiproliferative effect of auraptene in both ER + and ER− cells. It is noteworthy that we have shown auraptene to inhibit not only cell proliferation but also colony formation and invasiveness, which are valuable anticancer properties for this compound. It counteracted the stimulation of MCF-7 and SW-620 cell proliferation by E2 but induced a greater cell growth control than the ICI 164,384 antagonist that did not inhibit the ACAT activity of intact cells. Auraptene had an antigrowth effect on cell lines in the absence of stimulation by E2 that was comparable with the selective ACAT inhibitor TMP-153, showing the contribution of ACAT inhibition to the antigrowth effect.

In summary, we have identified two new targets for auraptene that are potentially responsible for its chemopreventive and anticancer action. The dual action of inhibiting ACAT and modulating the ER supports its application for the long-term treatment and prevention of cancer and offers a rationale for its evaluation in the treatment and the prevention of atherosclerosis and Alzheimer's disease.

References

Batetta B, Mulas MF, Sanna F, Putzolu M, Bonatesta RR, Gasperi-Campani A, Roncuzzi L, Baiocchi D, and Dessì S (2003) Role of cholesterol ester pathway in the control of cell cycle in human aortic smooth muscle cells. *FASEB J* **17:**746–748.

Booth C, Hargreaves DF, Hadfield JA, McGown AT, and Potten CS (1999) Isoflavones inhibit intestinal epithelial cell proliferation and induce apoptosis in vitro. *Br J Cancer* **80:**1550–1557.

Brzozowski AM, Pike AC, Dauter Z, Hubbard RE, Bonn T, Engström O, Ohman L, Greene GL, Gustafsson JA, and Carlquist M (1997) Molecular basis of agonism and antagonism in the oestrogen receptor. *Nature* **389:**753–758.

Curini M, Cravotto G, Epifano F, and Giannone G (2006) Chemistry and biological activity of natural and synthetic prenyloxycoumarins. *Curr Med Chem* **13:**199–222.

Curini M, Epifano F, Maltese F, Marcotullio MC, Tubaro A, Altinier G, Gonzales SP, and Rodriguez JC (2004) Synthesis and anti-inflammatory activity of natural and semisynthetic geranyloxycoumarins. *Bioorg Med Chem Lett* **14:**2241–2243.

de Medina P, Boubekeur N, Balaguer P, Favre G, Silvente-Poirot S, and Poirot M (2006) The prototypical inhibitor of cholesterol esterification, Sah 58–035 [3-[decyldimethylsilyl]-n-[2-(4-methylphenyl)-1-phenylethyl]propanamide], is an agonist of estrogen receptors. *J Pharmacol Exp Ther* **319:**139–149.

de Médina P, Favre G, and Poirot M (2004) Multiple targeting by the antitumor drug tamoxifen: a structure-activity study. *Curr Med Chem Anticancer Agents* **4:**491–508.

de Medina P, Paillasse MR, Segala G, Poirot M, and Silvente-Poirot S (2010) Identification and pharmacological characterization of cholesterol-5,6-epoxide hydrolase as a target for tamoxifen and AEBS ligands. *Proc Natl Acad Sci USA* **107:**13520–13525.

de Medina P, Payré B, Boubekeur N, Bertrand-Michel J, Tercé F, Silvente-Poirot S, and Poirot M (2009a) Ligands of the antiestrogen-binding site induce active cell death and autophagy in human breast cancer cells through the modulation of cholesterol metabolism. *Cell Death Differ* **16:**1372–1384.

de Medina P, Payré BL, Bernad J, Bosser I, Pipy B, Silvente-Poirot S, Favre G, Faye JC, and Poirot M (2004) Tamoxifen is a potent inhibitor of cholesterol esterification and prevents the formation of foam cells. *J Pharmacol Exp Ther* **308:**1165–1173.

de Medina P, Silvente-Poirot S, and Poirot M (2009b) Tamoxifen and AEBS ligands induced apoptosis and autophagy in breast cancer cells through the stimulation of sterol accumulation. *Autophagy* **5:**1066–1067.

Epifano F, Genovese S and Curini M (2008) Auraptene: phytochemical and pharmacological properties, in *Phytochemistry Research Progress* (Matsumoto T ed) pp 145–162, Nova Science Publishers, Inc., New York.

Galés C, Sanchez D, Poirot M, Pyronnet S, Buscail L, Cussac D, Pradayrol L, Fourmy D, and Silvente-Poirot S (2003) High tumorigenic potential of a constitutively active mutant of the cholecystokinin 2 receptor. *Oncogene* **22:**6081–6089.

Holbeck S, Chang J, Best AM, Bookout AL, Mangelsdorf DJ, and Martinez ED (2010) Expression profiling of nuclear receptors in the NCI60 cancer cell panel reveals receptor-drug and receptor-gene interactions. *Mol Endocrinol* **24:**1287–1296.

Janakiram NB, Steele VE, and Rao CV (2009) Estrogen receptor-beta as a potential target for colon cancer prevention: chemoprevention of azoxymethane-induced colon carcinogenesis by raloxifene in F344 rats. *Cancer Prev Res (Phila Pa)* **2:**52–59.

Jensen EV and Jordan VC (2003) The estrogen receptor: a model for molecular medicine. *Clin Cancer Res* **9:**1980–1989.

Jordan VC (2003) Tamoxifen: a most unlikely pioneering medicine. *Nat Rev Drug Discov* **2:**205–213.

Jordan VC (2004) Selective estrogen receptor modulation: concept and consequences in cancer. *Cancer Cell* **5:**207–213.

Jordan VC (2007) SERMs: meeting the promise of multifunctional medicines. *J Natl Cancer Inst* **99:**350–356.

Kedjouar B, de Médina P, Oulad-Abdelghani M, Payré B, Silvente-Poirot S, Favre G, Faye JC, and Poirot M (2004) Molecular characterization of the microsomal tamoxifen binding site. *J Biol Chem* **279:**34048–34061.

Kohno H, Suzuki R, Curini M, Epifano F, Maltese F, Gonzales SP, and Tanaka T (2006) Dietary administration with prenyloxycoumarins, auraptene and collinin, inhibits colitis-related colon carcinogenesis in mice. *Int J Cancer* **118:**2936–2942.

Krishnan P, Yan KJ, Windler D, Tubbs J, Grand R, Li BD, Aldaz CM, McLarty J, and Kleiner-Hancock HE (2009) Citrus auraptene suppresses cyclin D1 and significantly delays N-methyl nitrosourea induced mammary carcinogenesis in female Sprague-Dawley rats. *BMC Cancer* **9:**259.

Levenson AS and Jordan VC (1998) The key to the antiestrogenic mechanism of raloxifene is amino acid 351 (aspartate) in the estrogen receptor. *Cancer Res* **58:**1872–1875.

McDonnell DP, Clemm DL, Hermann T, Goldman ME, and Pike JW (1995) Analysis of estrogen receptor function in vitro reveals three distinct classes of antiestrogens. *Mol Endocrinol* **9:**659–669.

Ogawa K, Kawasaki A, Yoshida T, Nesumi H, Nakano M, Ikoma Y, and Yano M (2000) Evaluation of auraptene content in citrus fruits and their products. *J Agric Food Chem* **48:**1763–1769.

Ohnishi H, Asamoto M, Tujimura K, Hokaiwado N, Takahashi S, Ogawa K, Kuribayashi M, Ogiso T, Okuyama H, and Shirai T (2004) Inhibition of cell proliferation by nobiletin, a dietary phytochemical, associated with apoptosis and characteristic

gene expression, but lack of effect on early rat hepatocarcinogenesis in vivo. *Cancer Sci* **95:**936–942.

Paillasse MR, de Medina P, Amouroux G, Mhamdi L, Poirot M, and Silvente-Poirot S (2009) Signaling through cholesterol esterification: a new pathway for the cholecystokinin 2 receptor involved in cell growth and invasion. *J Lipid Res* **50:**2203–2211.

Payré B, de Medina P, Boubekeur N, Mhamdi L, Bertrand-Michel J, Tercé F, Fourquaux I, Goudounèche D, Record M, Poirot M, et al. (2008) Microsomal antiestrogen-binding site ligands induce growth control and differentiation of human breast cancer cells through the modulation of cholesterol metabolism. *Mol Cancer Ther* **7:**3707–3718.

Poirot M, De Medina P, Delarue F, Perie JJ, Klaebe A, and Faye JC (2000) Synthesis, binding and structure-affinity studies of new ligands for the microsomal antiestrogen binding site (AEBS). *Bioorg Med Chem* **8:**2007–2016.

Renoir JM, Bouclier C, Seguin A, Marsaud V, and Sola B (2008) Antioestrogen-mediated cell cycle arrest and apoptosis induction in breast cancer and multiple myeloma cells. *J Mol Endocrinol* **40:**101–112.

Shiau AK, Barstad D, Loria PM, Cheng L, Kushner PJ, Agard DA, and Greene GL (1998) The structural basis of estrogen receptor/coactivator recognition and the antagonism of this interaction by tamoxifen. *Cell* **95:**927–937.

Tanaka T, de Azevedo MB, Durán N, Alderete JB, Epifano F, Genovese S, Tanaka M, Tanaka T, and Curini M (2010) Colorectal cancer chemoprevention by 2 beta-cyclodextrin inclusion compounds of auraptene and 4′-geranyloxyferulic acid. *Int J Cancer* **126:**830–840.

Tanaka T, Kawabata K, Kakumoto M, Matsunaga K, Mori H, Murakami A, Kuki W, Takahashi Y, Yonei H, Satoh K, et al. (1998) Chemoprevention of 4-nitroquinoline 1-oxide-induced oral carcinogenesis by citrus auraptene in rats. *Carcinogenesis* **19:**425–431.

Tanaka T, Kohno H, Murakami M, Kagami S, and El-Bayoumy K (2000) Suppressing effects of dietary supplementation of the organoselenium 1,4-phenylenebis(methylene)selenocyanate and the Citrus antioxidant auraptene on lung metastasis of melanoma cells in mice. *Cancer Res* **60:**3713–3716.

Tosi MR and Tugnoli V (2005) Cholesteryl esters in malignancy. *Clin Chim Acta* **359:**27–45.

Vedin LL, Lewandowski SA, Parini P, Gustafsson JA, and Steffensen KR (2009) The oxysterol receptor LXR inhibits proliferation of human breast cancer cells. *Carcinogenesis* **30:**575–579.

Weige CC, Allred KF, and Allred CD (2009) Estradiol alters cell growth in nonmalignant colonocytes and reduces the formation of preneoplastic lesions in the colon. *Cancer Res* **69:**9118–9124.

Wittmann BM, Sherk A, and McDonnell DP (2007) Definition of functionally important mechanistic differences among selective estrogen receptor down-regulators. *Cancer Res* **67:**9549–9560.

Xu X and Thomas ML (1994) Estrogen receptor-mediated direct stimulation of colon cancer cell growth in vitro. *Mol Cell Endocrinol* **105:**197–201.

Zheng Q, Hirose Y, Yoshimi N, Murakami A, Koshimizu K, Ohigashi H, Sakata K, Matsumoto Y, Sayama Y, and Mori H (2002) Further investigation of the modifying effect of various chemopreventive agents on apoptosis and cell proliferation in human colon cancer cells. *J Cancer Res Clin Oncol* **128:**539–546.

Address correspondence to: Dr. Marc Poirot, INSERM U-563, Equipe métabolisme, oncogenèse et différenciation cellulaire, Centre de Physiopathologie de Toulouse Purpan, Institut Claudius Regaud, 20 rue du Pont Saint Pierre, 31052 Toulouse Cedex, France. E-mail: marc_poirot@hotmail.com